Numerical estimation of internal stress relieving in destructive test

Elżbieta Szymczyk, Agnieszka Derewońko, Grzegorz Sławiński, Jerzy Jachimowicz

Department of Mechanics and Applied Computer Science
Military University of Technology
ul. Kaliskiego 2, 00-908 Warsaw, Poland
e-mail: eszymczyk@wat.edu.pl

The paper deals with the analysis of residual stress fields in the riveted joint and the estimation of the internal stress magnitude releasing by partial and complete removing of the rivet material. Stress relieving causes deformations around the rivet hole, which can be measured and compared to the deformation state before removal. Numerical FE simulations of the upsetting process are carried out to determine the residual stress and strain fields. The contact with friction is defined between the mating parts of the joint. Non-destructive testing methods are used in combination with numerical calculations.

Keywords: riveted joint, FEM local model, destructive and non-destructive methods

1. INTRODUCTION

Aircraft structures, like airplane or helicopter fuselages, wings etc. are thin–walled structures, with coverings made of thin sheets stiffened by stringers, frames or ribs. Sheets are typically assembled by multiple riveted or bolted joints. Rivets and bolts are also used to join sheets and stiffeners. Therefore, fatigue resistance of the aircraft structure depends on tens of thousands or even hundreds of thousands riveted joints, which are used to build it [1].

Thin-walled constructions are made of metal sheets or composite covers. Aluminium or titanium alloys are commonly used in aviation. The aluminium alloy 2024T3 is considered in the paper.

The riveted joints are critical areas of the aircraft structure due to severe stress concentrations, plastic strain, secondary bending and effects such as surface damage (fretting wear). These phenomena cause initiation and propagation of fatigue crack and decrease fatigue resistance of the riveted joint [1, 2].

The residual stress (locally exceeding the yield stress level) and plastic strain states are generated in the joint after the riveting process. Residual stress can be defined as the stress state that remains in a part of the structure after all applied forces have been removed. Thermal and mechanical processes like heat treatment, hot or cold rolling, riveting etc. exert an influence on the level of residual stresses. The total stress experienced by the material at a given location within a structural component depends on the residual and applied stress. Residual stress fields are widely accepted to have a significant influence on fatigue life of riveted joints. Compressive residual stress can be beneficial because it tends to decrease the probability of stress corrosion and fatigue cracking [3–5].

Verification of numerical model requires experimental measurement in order to estimate actual stress distribution within a structural component. Stress is a complex tensor field that cannot be measured at a point, but over a finite gauge volume. Furthermore, residual stresses cannot be

measured directly, instead they can be calculated from other physical quantities like elastic strain, displacement, speed of sound or magnetic signature.

Measurement techniques can be divided into destructive and non-destructive ones. The destructive techniques are based on inferring the original stress from the displacement caused by relieving the stress due to material removing i.e. layer removal and contour method [6]. Non-destructive methods allow to measure some parameters related to the stress such as: elastic strain of atomic lattice planes (X-ray diffraction), magnetic properties, speed of sound, temperature etc. Conventional X-ray diffraction is limited to the depth of $5\,\mu$m so it is often applied in combination with destructive layer removal.

The paper deals with the numerical analysis of stress distribution in the neighbourhood of a driven rivet head before and after rivet material removal.

2. NUMERICAL MODEL

Analysis is carried out for a single lap riveted joint. The specimens are made of thin aluminium sheets connected by six mushroom rivets. The sheets are made of 2024T3 aluminium alloy and the rivet is made of PA25 alloy.

Materials used in riveted joints are subjected to high-strain deformation (plastic deformation). Mechanical tensile and compressive testing is required to determine mechanical property data. The sheet material (2024T3) is tested for a typical flat specimen (in PN-91/H-04310 standard). Tensile and compressive tests are performed also for the "rivet" sample. The average material properties obtained in laboratory tests are shown in Table 1.

Multilinear elasto-plastic true stress-logarithmic strain curves [7] (used in numerical calculations) for the rivet and sheet alloys are presented in Fig. 1.

FE simulations of the upsetting process are carried out using the MSC Marc code. The square part of sheets 10.5 mm wide surrounding a single mushroom rivet (shank diameter $r = 3.5$ mm) is considered. The local model geometry consists of three solids: a rivet and two sheets (Fig. 2), whereas FE mesh contains about 90 thousands eight-node, isoparametric, three-dimensional brick elements (type Hex8) with tri-linear interpolation function [7].

Table 1. Material properties

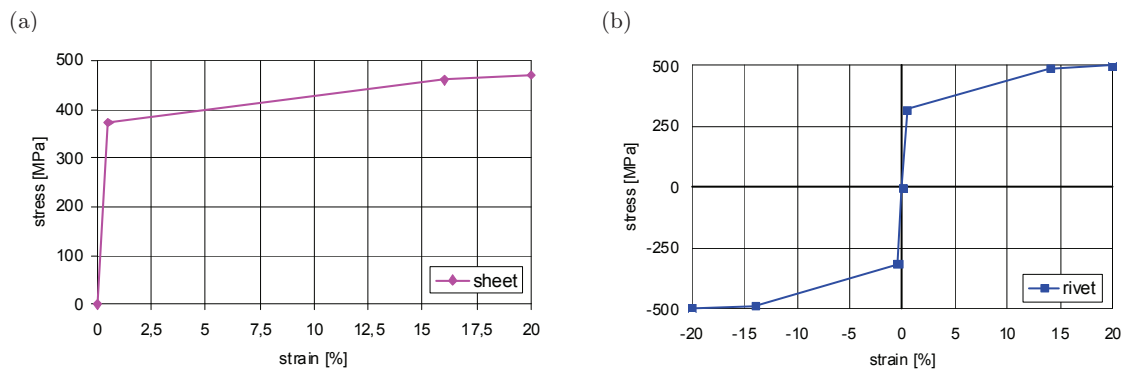| Material	Young modulus [MPa]	Poisson ratio [-]	Yield stress [MPa]	Ultimate stress [MPa]
Sheet (2024T3)	68000	0.3	374	460
Rivet (PA25)	71000	0.33	318	424

(a)

(b)

Fig. 1. Elasto-plastic stress-strain curves: (a) sheet, (b) rivet
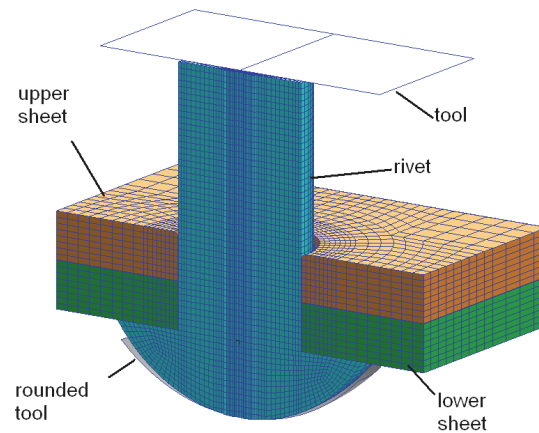
Fig. 2. Local model of riveted joint

The outside edges of the sheets are constrained in the normal direction so that the model describes a part of the multi-riveted joint. The rounded and flat rivet tools are assumed to be rigid surfaces. The rounded (lower) tool is fixed and the flat (upper) one is moved a given distance down.

The two load steps: the rivet squeezing (press and unloading) as well as partial and complete removing of the rivet material are studied.

The magnitude of the yield stress and tensile strength are obtained from uniaxial test and the yield value for the multiaxial state is calculated using the von Mises criterion. The classical updated Lagrange formulation (with large strain plasticity option) for elastic-plastic materials is used due to large geometrical and material non-linearities.

Contact (node-to-surface type) with friction is defined between the mating parts of the joint (7 areas in contact). The Coulomb model with trial friction coefficient $\mu = 0.2$ is used. This value has a significant influence on the shape of the driven rivet head [8]. During riveting the relative sliding between the rivet and the sheets is rather small. The penalty method is applied to numerical implementation of the contact constraints. Iterative penetration checking approach allows to change the contact condition within the Newton-Raphson iteration loop. Using this procedure, the iteration process is done simultaneously to satisfy both the contact constraints and global equilibrium using the Newton-Raphson method. This procedure is accurate and stable, but may require additional iterations.

3. SIMULATION OF RIVETING PROCESS

The local model is used to determine the residual stress and strain fields at the mushroom rivet and around the hole after riveting process as well as the resulting fields after partial and complete removing of the rivet material.

Deformation of the rivet are presented in Fig. 3. Nominal rivet head diameter is equal to 5.2 mm and its height achieve 1.8 mm (for 3.5 mm of rivet shank diameter).

Irreversible plastic deformations of the sheet material around the rivet hole (Fig 4) remain after the riveting process as a result of the rivet shank swelling in the hole. Strain concentrations occur under the driven rivet head and achieve maximum value 3.6%.

The absolute values of stresses in the upper sheet (from the side of the formed rivet head) are about 25% greater than corresponding values in the lower sheet (Fig. 5a). The extreme negative value of the radial stresses occur at the rivet hole (under the rivet head) and is equal to -452 MPa. After the rivet removal it decreases to -157 MPa (Fig. 5b).
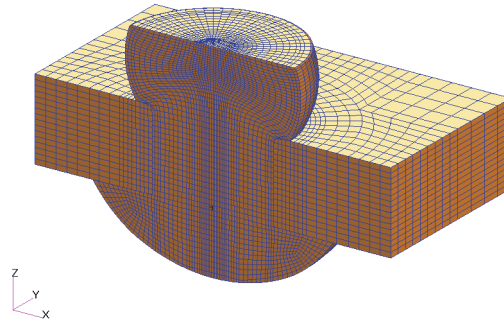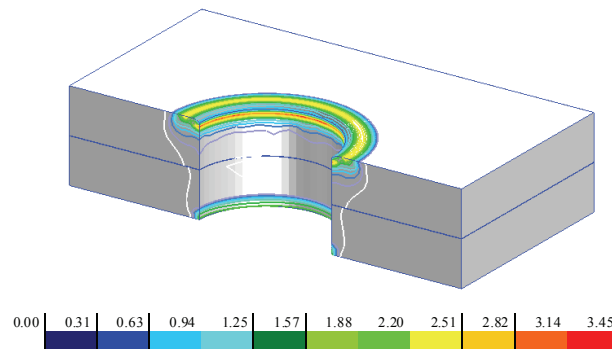
Fig. 3. Rivet deformation

| 0.00 | 0.31 | 0.63 | 0.94 | 1.25 | 1.57 | 1.88 | 2.20 | 2.51 | 2.82 | 3.14 | 3.45 |

Fig. 4. Residual plastic strain field

(a)   (b)

$\sigma_{\min} = -452 \, \mathrm{MPa}$ $\sigma_{\min} = -157 \, \mathrm{MPa}$

| 100 | 50 | 0 | -50 | -101 | -151 | -201 | -251 | -301 | -352 | -402 | -452 |

Fig. 5. Residual radial stress field: (a) after riveting, (b) after rivet removal

4. Results of rivet material removing

Non-destructive testing method (X-ray diffraction) is used for validation of numerical results. Comparison between numerical and experimental results for the sheet region a bit further from the driven rivet head gives a satisfactory agreement (Fig. 6). Points p1, p2 and p3 represent the radial stress values obtained by X-ray measurement [3]. Stress assessment in the sheets around the hole under the driven rivet head involves application of conventional X-ray diffraction in combination with destructive layer removal method. Deformation and stress states calculated numerically are presented in the paper and they will be compared with values measured in the specimen.
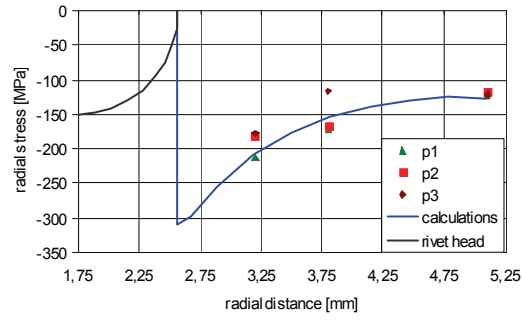
Fig. 6. Numerical and experimental results comparison
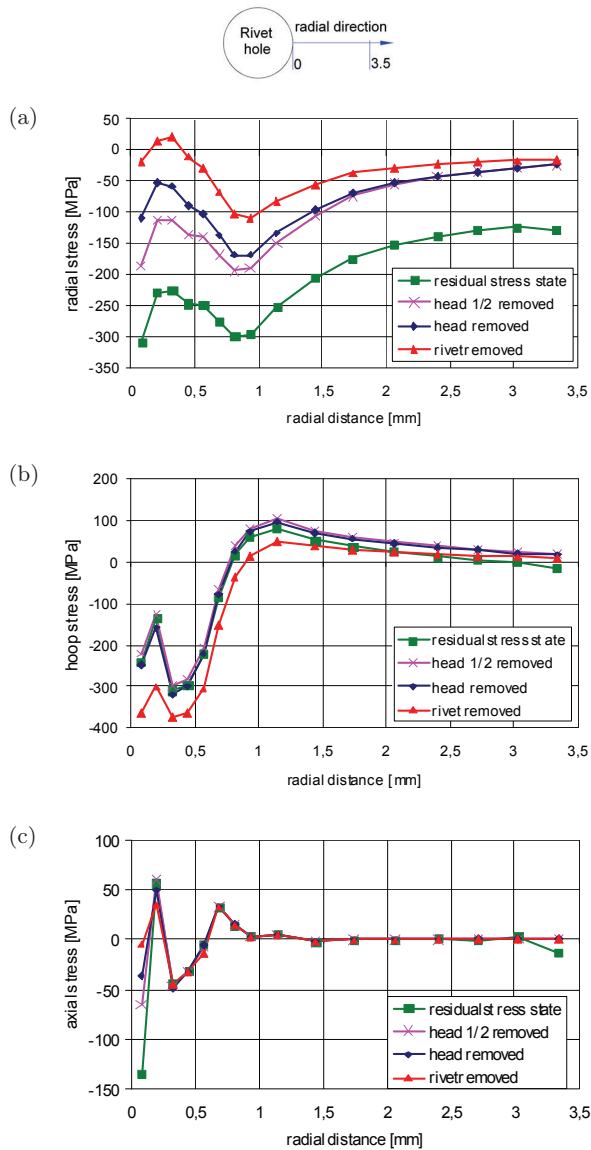

Fig. 7. Stress distribution vs. radial distance from the hole: (a) radial, (b) hoop, (c) axial component

Residual stress values versus radial distance from the hole are compared with resulting stresses after the partial (driven head only) and complete removal of the rivet material (Fig. 7).

The radial stress component is especially sensitive to rivet removing. Stress absolute values change (decrease) about 30% after half of rivet head removal, 40% after rivet head removal and consecutive 20% after the entire rivet removal.

The absolute values of the hoop stress component increase about 20% as a consequence of rivet removing and simultaneous decreasing of the rivet hole radius. Head material removing doesn't cause large changes in the hoop stress field.

The axial stress component variations take place only under the rived head and are proportional to the amount of rivet material removed.
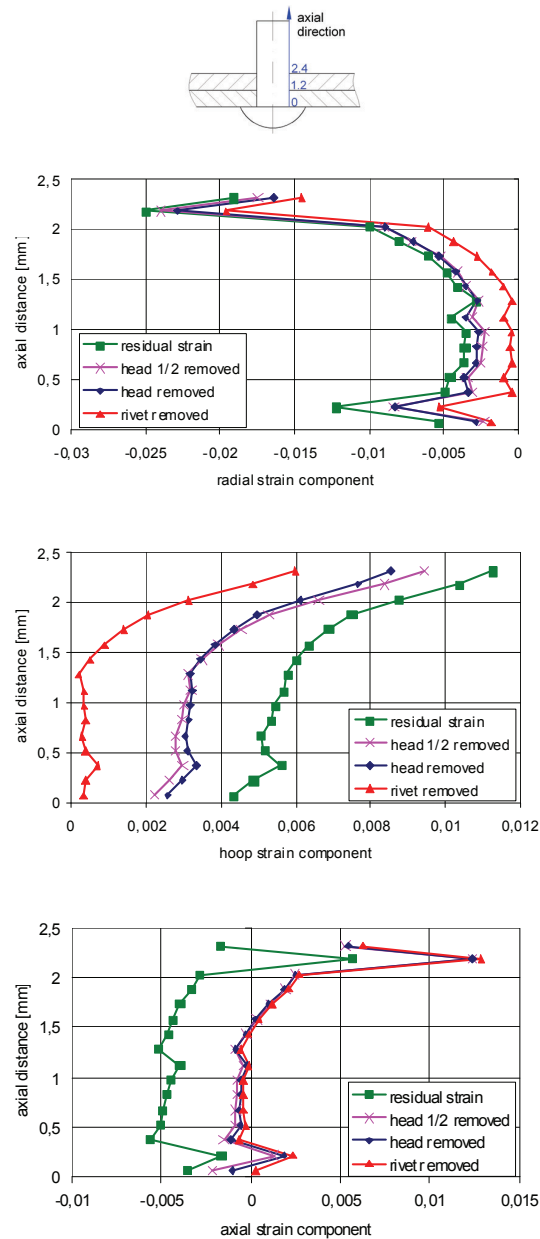

Fig. 8. Strain evolution vs. sheet axial distance

Strain evolution of the rivet hole after riveting process and during rivet material removing are presented in Fig. 8.

The radial component of residual strain is negative (it corresponds to radial compression) and during material removing the absolute value of this component is decreasing. The hoop component is positive (tension in hoop direction occurs) and it also decreases after rivet material removal. The axial component of residual strain is negative and its absolute value decreases to zero.

Radial displacement of the rivet hole after riveting process and during rivet material removing are presented in Fig. 9. After riveting the radial displacements of the rivet hole are 0.01 mm on the average. Head removing causes increasing of this component to 0.015 mm however whole rivet removal decreases it down to 0.005 mm.
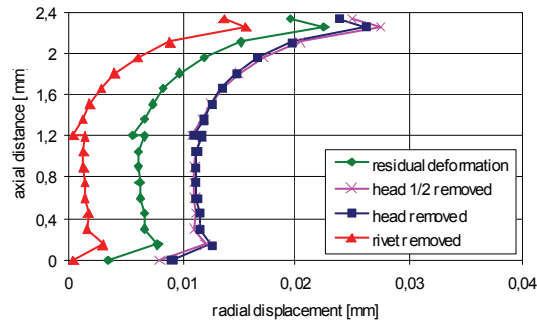

Fig. 9. Hole deformation vs. sheet axial distance

5. Conclusions

Numerical results are very sensitive to the used materials and the FE mesh parameters. If the element size is too large or the element shape is not appropriate then node penetrations in the contact area and non-physical stress concentrations occur in the riveted joint [2]. The analysis of stress and strain fields with respect to the mesh density and the element shape is presented in paper [8].

In the area of structure modelling some solutions to the problem connected with destructive test in riveted joints are proposed. The influence of the material removal on the resulting stress fields is analysed. Numerical simulations allow to investigate the stress and strain state in the joint during the riveting process and the service loading. The stress and strain field can be presented in the neighbourhood of a contact interface, where experimental detection and measurement is very difficult and expensive.

The radial stress component is very sensitive to rivet material removing, especially for the selected boundary conditions. Although radial stress absolute values decrease monotonically to 30% of residual stress after the entire rivet removal the head material removing doesn't cause large changes in the hoop stress field.

Radial deformation tends to increase during head removing and decrease after entire rivet removal. Deformation and stress states calculated numerically will be compared with values measured in the specimen.

REFERENCES

[1] J. de Rijck. *Stress Analysis of Fatigue Crack in Mechanically Fastened Joints.* Doc. Dissertation, Delft University of Technology, 2005.

[2] A. Arte. *A Finite Element and Experimental Investigation on the Fatigue of Riveted Lap Joint in Aircraft Applications.* Doc. Dissertation, Georgia Institute of Technology, 2006.

[3] E. Szymczyk, J. Jachimowicz, G. Sławiński. Analysis of residual stress fields in riveted joint. *Journal of KONES*, **14**: 465–474, 2007.

[4] E. Szymczyk, J. Jachimowicz, G. Sławiński. Riveting process simulation – upsetting of the mushroom rivet. *Journal of KONES*, **15**(2): 493–502, 2008.

[5] E. Szymczyk, J. Jachimowicz, G. Sławiński, A. Derewońko. Numerical modelling and analysis of riveting process in aircraft structure (in Polish). *Górnictwo odkrywkowe* **4**–**5**: 88–94, 2008.

[6] P.J. Withers . Recent advances in residual stress measurement. *Int. J. Pressure Vessels and Piping*, **85**: 118–127, 2008.

[7] *MSC Marc Theoretical Manual.* MSC Corp, 2007.

[8] A. Derewońko, E. Szymczyk, J. Jachimowicz. Numerical modelling of contact problem in the riveting process (in Polish). *Biuletyn WAT 04*, Vol. LV, pp. 89–100, 2006.